Interference, Coulomb blockade, and the identification of non-Abelian quantum Hall states

Ady Stern,[1] Bernd Rosenow,[2] Roni Ilan,[1] and Bertrand I. Halperin[3]
[1]*Department of Condensed Matter Physics, Weizmann Institute of Science, Rehovot 76100, Israel*
[2]*Max-Planck-Institute for Solid State Research, Heisenbergstr. 1, D-70569 Stuttgart, Germany*
[3]*Physics Department, Harvard University, Cambridge, Massachusetts 02138, USA*
(Received 21 December 2009; published 19 August 2010)

We study electronic-transport phenomena in a Fabry-Perot interferometer in the fractional quantum Hall regime in two limits. We analyze the lowest-order interference pattern in a nearly open interferometer (weak-backscattering limit) and the temperature dependence of the Coulomb-blockade transmission peaks in a nearly closed interferometer (strong-backscattering limit). For both limits, we consider two series of fractional quantized Hall states, one with Abelian and one with non-Abelian quasiparticles. We show that the results obtained in the two limits give identical information about the quasiparticle statistics. Although the experimental signatures of the Abelian and non-Abelian states may be similar in some circumstances, we argue that the two cases may be distinguished due to the sensitivity of the Abelian states to local perturbations, to which the non-Abelian states are insensitive.

DOI: 10.1103/PhysRevB.82.085321 PACS number(s): 73.43.−f, 73.23.Hk, 73.63.Kv, 85.35.Ds

I. INTRODUCTION

Much effort has been devoted in recent years to the search for experimental demonstrations of the exotic quantum statistics of quasiparticles (QPs) in the fractional quantum Hall effect (QHE). Experiments were proposed, and some have been carried out, or attempted. Among these there are several that are based on the quantum Hall analog of the Fabry-Perot (FP) interferometer, either through interference[1–6] or through the Coulomb blockade (CB).[2,6,7] In particular, interference and Coulomb blockade were predicted to show rather robust signatures of non-Abelian statistics in quantum Hall states that are believed to be non-Abelian. Recent data on a Fabry-Perot interferometer at the $\nu=5/2$ state may be a first confirmation of these predictions.[8]

In the context of the QHE, a Fabry-Perot interferometer, shown schematically in Fig. 1, is a Hall bar perturbed by two constrictions (quantum point contacts—QPCs).[9] The two QPCs introduce amplitudes for interedge tunneling of quasiparticles. The quantity of interest is the probability of backscattering, as a function of magnetic field and the interferometer's area. When the amplitudes for interedge tunneling are small, the probability for backscattering involves the interference of two trajectories. When the amplitudes are large, the interferometer is almost closed, and its interior becomes a quantum dot. The probability for backscattering is then close to unity, except in the vicinity of Coulomb-blockade transmission peaks. The transition between the two limits—the "lowest-order interference" and "Coulomb-blockade" limits—may be tuned by adjusting the tunneling amplitudes of the two point contacts.

The expected dependence of the backscattered current I on the magnetic field B and the interferometer's area A for non-Abelian QHE states was calculated in several works.[2–6] Unique signatures were predicted, that originate from the non-Abelian nature of the states. These signatures all emerged from a model in which the bulk of the interferometer houses a number of localized quasiparticles, n_{is}. The anyonic statistics associated with the edge current that encircles these quasiparticles modifies the interference contribution to the backscattered current. The model assumes that the area of the interferometer may be varied by means of a voltage applied to a gate, and the number n_{is} may be varied by means of a magnetic field. Furthermore, the model assumes that the density of quasiparticles is sufficiently low such that the n_{is} quasiparticles localized in the bulk are far

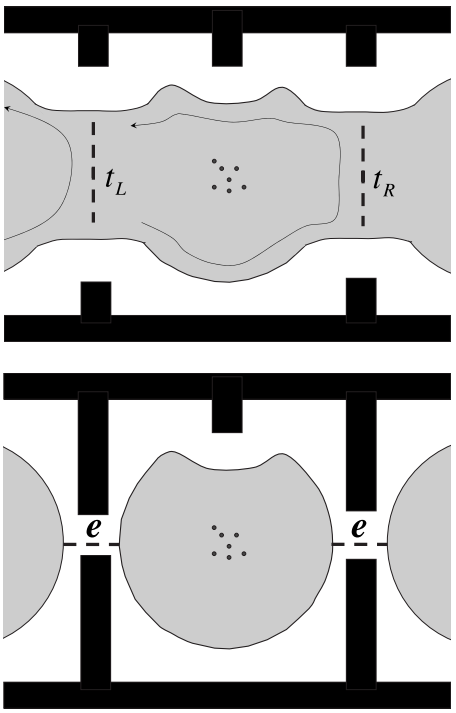

FIG. 1. A sketch of the Fabry-Perot interferometer. The upper figure shows the interferometer in the lowest-order interference limit. Quasiparticles tunnel from one edge to the other at the two QPCs and the two interfering trajectories appear above. The lower figure shows the interferometer in the Coulomb-blockade regime, where the QPCs are closed and only electrons are allowed to tunnel through the dot.

enough from the edge for their coupling to the edge to be negligible. The area of the interferometer is assumed not to vary with the variation in a magnetic field. Finally, the model assumes that the backscattered current primarily originates from tunneling of quasiparticles whose charge is the smallest one possible, and whose tunneling is most relevant (in the renormalization-group sense). The applicability of these assumptions to the systems used in current experiments and the effect of deviations from these assumption are a subject of current experimental[10,11] and theoretical[12–14] studies. For the present study, we adopt this model.

In this work, we first study $I(B,A)$ in the limits of lowest-order interference and of Coulomb blockade. We find that the two limits give the same information regarding the state they probe. We then get an insight to the relation between the two limits by focusing on a Coulomb-blockaded interferometer and studying the thermally averaged number of electrons in the interferometer $\mathcal{N}(B,A,T)$ as a function of the field B, the area A, and the temperature T. At low temperature, $\mathcal{N}$ is an integer that rises in steps when the area is increased, and the derivative $\partial\mathcal{N}/\partial A$ shows a series of peaks. The maxima in the derivative coincide with the Coulomb-blockade peaks in the conductance through the dot. As the temperature rises, these peaks are smeared into a sinusoidal pattern. We find the dependence of this sinusoidal pattern on the properties of the quantum Hall state to be identical to that found in $I(B,A)$ in the lowest-order interference limit.

Generally, the discrete spectrum of a quantum dot is a result of a Bohr-Sommerfeld interference of infinitely-many trajectories. At low temperature, a small number of energy states is probed and many trajectories interfere. As the temperature gets high, interference of trajectories that encircle the dot many times is smeared, until eventually only lowest-order trajectories are left. The unique properties of the quantum Hall states that we examine, both Abelian and non-Abelian, allow us to relate the two limits. Remarkably, although the energy states of the closed dots are all characterized by an integer number of electrons, the high-temperature behavior of $\mathcal{N}(B,A)$ reflects the properties of the quasiparticle with lowest charge.

Following a recent work by Bonderson *et al.*,[15] we also examine the level of unambiguity with which the Fabry-Perot interferometer is able to identify a non-Abelian quantum Hall state, namely, we examine whether the same experimental signatures may result from states that are Abelian as well as non-Abelian. Bonderson and collaborators have shown that the zero-temperature Coulomb-blockade peak patterns that are predicted for the non-Abelian Read-Rezayi series of states are identical to the ones predicted for the Abelian series of multicomponent Halperin states.[15] We show that for the most prominent candidate for a non-Abelian state, $\nu=5/2$, the same identity of patterns holds also for Fabry-Perot interference experiments and for finite-temperature Coulomb-blockade experiments. Largely, this holds also for the more complicated states at $\nu=2+\frac{k}{k+2}$ with $k>2$, although in this case subtle differences exist in the interference signals between the Abelian multicomponent Halperin states and the non-Abelian Read-Rezayi states.

The identity of the predictions for these two series of Abelian and non-Abelian states is based on a very limiting assumption regarding the Abelian states. The Abelian multicompnent states of $\nu=2+\frac{k}{k+2}$ are composed of k flavors of electrons, and their similarity to the non-Abelian Read-Rezayi states holds only under a full symmetry between all the flavors. A breaking of that symmetry affects the Coulomb blockade and interference patterns and distinguishes the Abelian and non-Abelian states.[15] In the $k=2$ case, corresponding to the $\nu=5/2$ state, the two flavors of electrons are likely to be the two spin states. The symmetry between the two states would then be broken by the Zeeman coupling of the spin to the magnetic field or by spin-orbit coupling. In contrast, the patterns predicted for the non-Abelian states enjoy the insensitivity characteristic of these states to local perturbations. For the $k>3$ cases, there are no obvious degrees of freedom that lead to the electronic system splitting into k flavors but we find the comparative analysis of the multicomponent Halperin states and the Read-Rezayi states to be of theoretical interest. Again, predictions for the Abelian and non-Abelian series of states are very similar at the point of exact symmetry between the k flavors, and differ as this symmetry is broken. Again, the Abelian states are sensitive to local perturbations while the non-Abelian ones are not. We note that both Abelian and non-Abelian states are sensitive to a coupling between the localized bulk quasiparticles and the chiral neutral modes, as discussed in Refs. 12–14.

The structure of the paper is as follows: in Sec. II, we analyze the $\nu=5/2$ case. We examine two candidate states for which the Coulomb-blockade signatures were found to be identical, the Pfaffian and the Halperin (3,3,1) state. We show that the same holds for the interference pattern as well, and comment on the subtle differences between the two states, differences that hold for both the Coulomb blockade and the interference experiments. In Sec. III, we analyze the $\nu=2+\frac{k}{k+2}$ series. We compare the Read-Rezayi series[16] to the multicomponent Halperin state series,[17] and show that the similarity in Coulomb-blockade patterns, discovered in Ref. 15, largely holds also for the FP interference. In Sec IV, we study a Coulomb-blockaded quantum dot and ask how the thermally averaged number of electrons in the dot $\mathcal{N}(B,A)$ depends on the field B, the area A, and the temperature T.

II. INTERFERENCE SIGNALS IN THE $\nu=5/2$ STATE

The two leading candidate states for a non-Abelian $\nu=5/2$ phase, the Pfaffian[18] and the anti-Pfaffian,[19,20] have been predicted to show a unique behavior in an FP device, in both limits. In the limit of lowest-order interference,[2,3] the pattern depends crucially on the parity of n_{is}. For an odd n_{is}, no interference signal is to be seen, i.e., the backscattered current would show no periodic dependence on the area of the interferometer. For an even n_{is} a periodic dependence should be observed, with the phase of the interference pattern assuming one of two possible values, mutually shifted by π. The phase chosen depends on the topological charge of the n_{is} localized quasiparticles. In the Coulomb-blockade limit[2] the area spacing between two consecutive Coulomb-blockade peaks depends on the parity of n_{is}. For odd n_{is}, the peaks are equally spaced while for even n_{is} they bunch into pairs.

These predictions are rather unique, being different from those expected for states of the integer QHE and simple fractional QHE states.[9,21,22] However, they alone do not identify the $\nu=5/2$ state as non-Abelian since another candidate state, the (3,3,1) state,[23] shares the same features. It was already shown that the Coulomb-blockade patterns of the Pfaffian, anti-Pfaffian, and the (3,3,1) are identical.[15] We now show that the same holds for the lowest-order interference.

The (3,3,1) state is a paired state characterized by a K matrix[24] of the form

$$K = \begin{pmatrix} 3 & 1 \\ 1 & 3 \end{pmatrix} \tag{1}$$

with the quasiparticle operators characterized by the vectors $l_\uparrow=(1,0)$ and $l_\downarrow=(0,1)$. The n_{is} quasiparticles are characterized by the vector $n=(n_\uparrow,n_\downarrow)$, with $n_{is}=n_\uparrow+n_\downarrow$. When an l_i (with $i=\uparrow,\downarrow$) quasiparticle encircles the bulk quasiparticles it accumulates a phase of $2\pi l_i K^{-1} n$. The incoming current is spin unpolarized, and thus the observed interference pattern is the sum of two patterns, whose phase difference is

$$2\pi(l_\uparrow - l_\downarrow)K^{-1}n = \pi(n_\uparrow - n_\downarrow). \tag{2}$$

When n_{is} is odd, this phase difference is an odd multiple of π. The two patterns then mutually cancel, leading to no periodic dependence on area. In contrast, for n_{is} even, the two patterns interfere constructively, and an interference pattern is to be seen. Furthermore, for an even n_{is} either $n_\uparrow,n_\downarrow$ are both even or both are odd. Interestingly, the interference patterns that result in these two cases are mutually shifted by π. These characteristics of the interference patterns are the same as those of the non-Abelian states—vanishing interference for an odd n_{is}, and two possible interference patterns, mutually shifted by π, for even n_{is}.

Just as in the case of the Coulomb blockade, the interference patterns described above for the (3,3,1) crucially depend on the symmetry between up and down spins. Any deviation from this symmetry, for example, in having a polarized incoming current or a Zeeman splitting between the two types of localized quasiparticles, would affect both the Coulomb-blockade peaks and the interference patterns. This is in an important contrast to the non-Abelian Pfaffian state in which the unique Fabry-Perot signatures are robust. For example, the vanishing lowest-order interference in the case of odd n_{is} results in the (3,3,1) case from the addition of two interference patterns, corresponding to the two spin directions. If the two are not of equal weight, they do not sum to zero. In contrast, in the Pfaffian case, the vanishing of the interference for odd n_{is} results from the fusion of two σ operators in the Ising conformal field theory (CFT) to equal weights of 1 and ψ particles, whose interference patterns are mutually shifted by π.[3] The equal weight of the two patterns is in this case inherent to the description of the state by the Ising CFT.

III. INTERFERENCE SIGNALS FOR THE $\nu=2+\frac{k}{k+2}$ STATES

Intriguing candidate description for filling factors $\nu=2+\frac{k}{k+2}$ are the Read-Rezayi states.[16] These states have been predicted to have their own unique characteristics in FP experiments.[4,6,7] In the limit of lowest-order interference, the observed interference pattern depends on the topological charge l of the n_{is} quasiparticles localized in the bulk. For each value of n_{is}, there are several possible integer values of the topological charge. For odd k, there are $(k+1)/2$ possible values of l. For even k, there are either $k/2$ or $\frac{k}{2}+1$ possible values depending on whether n_{is} is odd or even. The amplitude $I(l)$ of the interference term depends on l, being

$$I(l) = \frac{\cos\dfrac{\pi(l+1)}{k+2}}{\cos\dfrac{\pi}{k+2}}. \tag{3}$$

As for the Coulomb-blockade limit,[7] the positions of the Coulomb-blockade peaks as a function of the interferometer area depend on the topological charge, as different patterns of bunching of peaks are observed for different values of l.

Again, the Coulomb-blockade peak spacings predicted for the Read-Rezayi states are identical to those predicted for the multicomponent Halperin states. In view of the analogy described above between the Coulomb blockade and lowest-order interference for the $k=2$ case, it is natural to examine the lowest-order interference pattern expected for the multicomponent Halperin state for a particular k. The analysis starts from the K matrix, which is now a $k\times k$ matrix, whose elements satisfy $K_{ij}=1+2\delta_{ij}$, in a basis in which the charge vector t satisfies $t_i=1$ for all $i=1,\ldots,k$. The state of the bulk is now described by a vector $n=(n_1,\ldots,n_k)$ with $\Sigma_{i=1}^{k} n_i=n_{is}$. The most relevant quasiparticles are described by the vectors $l^{(j)}$ $(j=1,\ldots,k)$, with the elements of the vector $l^{(j)}$ being all zero, except the jth element, which is one: $l^{(j)}=(0\ldots0,1,0\ldots0)$. The phase accumulated by a quasiparticle $l^{(j)}$ encircling the bulk is

$$2\pi l^{(j)} K^{-1} n = -\pi\frac{n_{is}}{(k+2)} + \pi n_j. \tag{4}$$

As seen in this expression, the phases accumulated by different types of quasiparticles are identical, *up to a possible shift of* π. For a quasiparticle of type $l^{(j)}$, this shift is present for odd n_j and absent for even n_j. Again, if the incoming current does not break the symmetry between the k types of electrons, then the observed interference pattern will be a sum of k patterns, some of which are π shifted with respect to the rest. If the vector n is made of N_e even numbers and N_o odd numbers (with $N_e+N_o=k$ and both non-negative), and if we normalize the amplitude of the combined interference pattern to be 1 for the case $N_e=k$, then the amplitude of the interference pattern for the case where the bulk is described by a vector n is

$$I(n) = \frac{k - 2N_o}{k}. \tag{5}$$

The number of possible values for $I(n)$ depends on the parity of k and the parity of the number of bulk quasiparticles n_{is}. In principle, there are $k+1$ possible values for N_o but since $\Sigma_{i=1}^{k} n_i = n_{is}$, the parity of N_o is the parity of n_{is}. Thus, for k odd, there are $(k+1)/2$ possible values of $I(n)$ for each value of n_{is}. For k even there are $\frac{k}{2}+1$ possible values for $I(n)$ when n_{is} is even, and $k/2$ values when it is odd. Remarkably, this is precisely the number of possible values of $I(n)$ that are found in the lowest order interference pattern for the Read-Rezayi states [see Eq. (3) and the discussion around it].

As in the $k=2$ case, then, for all values of k the number of possible amplitudes for the interference pattern is the same for the multicomponent Halperin states and the Read-Rezayi states. For $k \geq 3$ there is, however, a difference between the amplitudes to be observed in the two states, as reflected in the difference between Eqs. (3) and (5). And again, the results presented here for the generalized Halperin state all depend on the symmetry between the k species of electrons, and thus lack the robustness of the corresponding results for the Read-Rezayi states.

IV. FINITE-TEMPERATURE COULOMB BLOCKADE

In this section, we study an interferometer in the Coulomb-blockaded limit, i.e., a quantum dot, and ask how the thermally averaged number of electrons within the interferometer $\mathcal{N}$ and its derivative $\frac{\partial \mathcal{N}}{\partial A}(B,A,T)$ depend on the magnetic field, area and temperature. In the limit $T=0$, the number of electrons on the dot is quantized to an integer, and $\frac{\partial \mathcal{N}}{\partial A}(B,A,T)$ shows Coulomb-blockade peaks as a function of the area A. These peaks may be smeared either by opening the point contacts that define the dot, approaching the lowest-order interference limit discussed in previous sections, or by raising the temperature, as we discuss now. In the analysis below, we assume that the edge is fully decoupled from the bulk, such that the state of the quasiparticles in the bulk remains constant for a time long enough for the measurement to take place while the state of the edge is in thermal equilibrium with its environment.

We start by studying $\frac{\partial \mathcal{N}}{\partial A}(B,A,T)$ for multicomponent Halperin states, and continue with the Read-Rezayi states. For both types of states at zero temperature, the peaks are unevenly spaced. In the intermediate temperature regime, where the temperature is lower than the dot's charging energy but higher than the typical energy for the dot's neutral modes, the peaks are well defined, yet they are broadened and shift toward equal spacing. When the temperature increases further to exceed the dot's charging energy, the peaks are smeared, and $\frac{\partial \mathcal{N}}{\partial A}(B,A,T)$ shows only small oscillations as a function of the area. This behavior is illustrated in Fig. 2. As we show below, both the deviation of the peaks from equal spacing in the intermediate temperature range and the small oscillations in the high-temperature regime carry the same information on the state of the system as the lowest-order interference discussed in the previous sections.

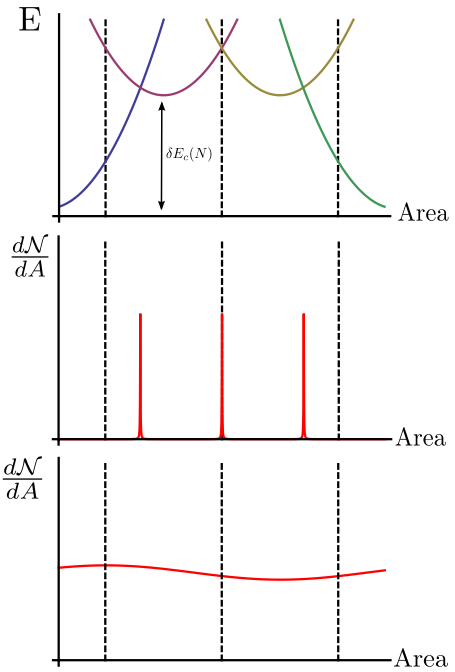

FIG. 2. (Color online) The behavior of $\frac{\partial \mathcal{N}}{\partial A}(B,A,T)$ as a function of area in three different temperature regimes. In the low- and intermediate temperature regimes, the electron number N is well quantized. The upper graph plots the energy parabolas, each of which corresponds to a different value of N. The contribution δE_c of Eq. (17) is indicated. Peaks in $\frac{\partial \mathcal{N}}{\partial A}(B,A,T)$ occur at crossing points of the parabolas. These points are unevenly spaced due to δE_c (middle graph, solid lines). In the intermediate temperature regime, the peaks are broadened and shift toward even spacing (the dashed lines indicate the limit of even spacing). In the high-temperature regime (the lower graph), the peaks are smeared to small oscillations. The plots use the case $k=3$, $n_{is}=0$ as an illustration.

A. Multicomponent Halperin states

Generally, the Hamiltonian density for an Abelian multiedge quantum Hall state is of the multi Luttinger liquid form,

$$\mathcal{H} = \frac{1}{4\pi} \sum_{ij} V_{ij} \left(\partial_x \phi_i - \frac{\Phi_i}{L} \right) \left(\partial_x \phi_j - \frac{\Phi_j}{L} \right), \tag{6}$$

where the equilibrium values Φ_i/L are determined by the magnetic field and the area enclosed by the edge. Unless otherwise defined, sums go over the range $1, \ldots, k$. The fields ϕ_j satisfy the commutation relations,

$$[\phi_i(x), \partial_x \phi_j(x')] = 2\pi K_{ij}^{-1} \delta(x - x'). \tag{7}$$

In the absence of bulk quasiparticles, the boundary conditions of the ϕ fields are

$$\phi_i(x + L) = \phi_i(x) + 2\pi m_i \tag{8}$$

with m_i integers. The symmetry between the different k electron flavors, together with the Hall conductance being $k/(k+2)$, requires the equilibrium values of $\partial_x \phi_i$, to satisfy $\frac{\Phi_i}{L} = \frac{BA}{L(k+2)\phi_0}$, independent of i. We will keep on using the notation Φ but omit the subscript. Furthermore, the symmetry

implies a high degree of symmetry for V_{ij}. Here we take $V_{ij}=V_1+V_2\delta_{ij}$. The energy corresponding to a set $\{m_i\}$ of winding numbers is

$$E(\{m_i\}) = \frac{\pi V_1}{L}\left[\sum_i (m_i-\Phi)\right]^2 + \frac{\pi V_2}{L}\sum_i (m_i-\Phi)^2. \quad (9)$$

There are k-electron creation operators whose scaling dimensions are lowest. These operators are $e^{il^{(j)}K\phi}$ with $j=1,\ldots,k$. Each of these operators changes the winding number m_j by 1.

The bulk quasiparticles introduce a shift in the boundary conditions of these fields, making them

$$\phi_i(x+L) = \phi_i(x) + 2\pi m_i + 2\pi l^{(i)}K^{-1}n \quad (10)$$

with the vector n describing the bulk quasiparticles. This shift may be understood by noting that when the quasiparticles of the vector n are created in the bulk, the state of the edge is affected by a creation operator that is a superposition of operators of the type $e^{in_i\phi_i(x)}$ for different positions x's. For every position x, this operators leads to the shift [Eq. (10)]. In the presence of that shift, the energies [Eq. (9)] change to

$$E(\{m_i\}) = \frac{\pi V_1}{L}\left[\sum_i (m_i-\Phi-l^{(i)}K^{-1}n)\right]^2 + \frac{\pi V_2}{L}\sum_i (m_i-\Phi - l^{(i)}K^{-1}n)^2. \quad (11)$$

As seen in Eq. (11), the very same term $l^{(i)}K^{-1}n$ that introduced a phase to the wave function of the interfering quasiparticle in the limit of lowest-order interference appears now as a flux shifting the energy for adding electrons to the edge in the limit of a closed dot.

With the spectrum at hand, we now analyze the thermodynamics of a closed dot as a function of temperature and area. In particular, we look at the way the average number of electrons $\mathcal{N}(A,T)$ on the dot depends on area A and the temperature T. The average $\mathcal{N}$ is calculated thermodynamically by summing over all configurations $\{m_j\}$. For a configuration $\{m_j\}$, the number of electrons on the edge of the dot is $N(\{m_j\})\equiv\Sigma_j m_j$. It is useful to express $\mathcal{N}$ in terms of the canonical-ensemble partition function Z_N, in which the contributing configurations all have $N(\{m_j\})=N$,

$$Z_N \equiv \sum_{\{m_j\}} \exp -\frac{E(\{m_j\})}{T}\delta_{N,N(\{m_j\})}. \quad (12)$$

The thermodynamical average $\mathcal{N}$ is then

$$\mathcal{N} = \frac{\sum_N NZ_N}{\sum_N Z_N}. \quad (13)$$

At zero temperature, $\mathcal{N}$ is the integer number of electrons $(\Sigma_i m_i)$ that minimizes the energy [Eq. (11)]. When this number changes, a Coulomb-blockade peak appears.

There are two energy scales that define the temperature regimes in the problem. The lower one is the scale of neutral degrees of freedom, V_2/L, and the higher one is the scale associated with charging energy, V_1/L. For a temperature that is much lower than both scales, we can approximate $T\approx 0$.

In the intermediate regime $\frac{V_1}{L}\gg T\gg\frac{V_2}{L}$, the number of electrons on the dot is still approximately quantized but many configurations $\{m_i\}$ contribute. For an area A for which the number of electrons on the dot is quantized to a value N_0, the partition function of the dot Z_{N_0} may be calculated in the canonical ensemble, and involves a summation over all internal states of the dot under the constraint that its total number of electrons is N_0. For an area A for which the dot is close to a transition from $\mathcal{N}=N_0$ to $\mathcal{N}=N_0+1$ the sum in Eq. (13) includes only the terms N_0 and N_0+1 and we have

$$\mathcal{N} = N_0 + \frac{Z_{N_0+1}}{Z_{N_0}+Z_{N_0+1}}. \quad (14)$$

We calculate Z_N in the Appendix. We find it convenient to write it in a form that highlights the contribution of the neutral mode. We find

$$Z_N \approx \frac{2\pi}{\sqrt{k}}\left(\frac{TL}{V_2}\right)^{(k-1)/2}\exp -\frac{E_c(N)+\delta E_c(N)}{T}. \quad (15)$$

In Eq. (15), the prefactor does not depend on N, and hence does not affect our calculation of $\mathcal{N}$. This prefactor originates from the entropy associated with the different configurations of the neutral mode. Within the exponential factor, E_c is the charging energy in the absence of a neutral mode,

$$E_c(N) = \frac{\pi}{L}\left(V_1+\frac{V_2}{k}\right)\left[N-\sum_j\left(\frac{1}{k+2}\frac{BA}{\Phi_0}+l^{(j)}K^{-1}n\right)\right]^2 \quad (16)$$

and δE_c is

$$\delta E_c = -2TkI(n)e^{-\pi TL(1-1/k)/V_2}\cos\left(2\pi\frac{N}{k}-\pi\frac{n_{is}}{k}\right). \quad (17)$$

The factor $e^{-\delta E_c/T}$ originates from the $\mathcal{N}$-dependent energy and entropy that come out of the different configurations of the neutral mode associated with the same electron number.

As evident from Eqs. (14) and (15), the center of the peak in $\frac{\partial\mathcal{N}}{\partial A}$ is at the area for which $E_c(N)+\delta E_c(N)=E_c(N+1)+\delta E_c(N+1)$ (see upper graph of Fig. 2). As seen in Eq. (17), the neutral mode contribution δE_c, which is on the order of V_2/L at zero temperature, becomes exponentially small at the intermediate temperature regime, and the peaks in $\frac{\partial\mathcal{N}}{\partial A}$ approach equal spacing, with the correction to equal spacing being exponentially small in TL/V_2. The correction oscillates with the number of electrons on the dot, with a period of k electrons, and depends on the state of the bulk quasiparticles through the factor $I(n)$, the same factor that appears in the lowest order interference term, see Eq. (5).

When the temperature is higher than the charging energy, $\mathcal{N}$ is not quantized. The thermally averaged $\mathcal{N}$ may be calculated through the standard methods to be

$$\mathcal{N} = \frac{k}{k+2}\frac{BA}{\Phi_0} + \mathcal{N}_1\left(\frac{BA}{\Phi_0}\right) - \frac{2TLI(n)}{V_1 + V_2/k} \times e^{-\pi TL/[k^2(V_1+V_2/k)]-\pi TL(1-1/k)/V_2} \sin\left(\frac{2\pi BA}{(k+2)\Phi_0} - \frac{\pi n_{is}}{k+2}\right) \tag{18}$$

with $I(n)$ the interference visibility, whose definition and properties are given at and below Eq. (5). In this expression the first term is the uniform linear increase in the charge with area, for a fixed density. The second and third terms are corrections that fall off exponentially in the limit of high temperature. The second term results from discreteness of the charge but is insensitive to the neutral modes (i.e., it is independent of V_2). The period of this term is an area increase that corresponds to a single electron. The third term is the one that we are interested in. The quasiparticle properties reflected in this term are precisely those that are reflected by the interference phase, Eq. (4). This limit is illustrated in the bottom graph of Fig. 2.

B. Read-Rezayi states

A similar calculation may be carried out for the non-Abelian Read-Rezayi states. Explicit expressions for the partition function are cumbersome. However, their low-temperature and high-temperature limits are rather easy to calculate. In fact, the two limits are related by a remarkable set of identities, derived by Cappelli *et al.* in Eq. (23), based on the modular invariance of the partition functions of the edge theory of the Read-Rezayi states.

The partition function for an edge of a Read-Rezayi state depends on the state of the bulk, and is characterized by two quantum numbers, n_{is}, l. Neglecting normalization factors that do not depend on these quantum numbers,[21]

$$Z^l_{n_{is}} = \sum_{p=-\infty}^{\infty}\sum_{b=1}^{k} \exp\left(-\frac{\pi V_1(k+2)}{TL} \times \frac{\left[pk + b - \frac{n_{is}}{k+2} - \frac{k}{k+2}\frac{BA}{\Phi_0}\right]^2}{k}\right)\chi^l_{n_{is}+2b}(T). \tag{19}$$

This expression is an analog to Eq. (13). However, while for the multicomponent states we had to sum over k quantum numbers, one per each edge state, for the Read-Rezayi states there are only two edge modes, one charged and one neutral. The two sums in Eq. (19) combine to a sum over all possible charges on the charged mode. The parafermionic character of the neutral part χ^l_m includes a sum over all internal states of the neutral mode. It is periodic as a function of m, with a period of $2k$. The parameter l is an integer in the range $0 \le l \le k$, and $n_{is}+l$ is an even number.

In the absence of the χ factor, $Z^l_{n_{is}}$ is a partition function of a single chiral Luttinger liquid, where the number of electrons on the dot is $kp+b$, the number of quasiholes in the bulk is n_{is}, and the charge of a quasihole is $1/(k+2)$. The character of the neutral part depends on two quantum numbers. One of them, l, depends only on the state of the bulk while the other depends also on the number of electrons in the dot, as reflected in the factor $n_{is}+2b$.

In the limit of $T \to 0$, the partition function is relatively easy to calculate. The contribution of the neutral part of the edge is

$$\chi^l_m(T) = \exp\left(-\frac{\epsilon^{m,l}_{gs}}{T}\right), \tag{20}$$

where $\epsilon^{m,l}_{gs}$ is the ground-state energy of the edge in the topological sector defined by m, l. The ground-state energy is dictated by the conformal field theory that describes the edges of Read-Rezayi states, Z_k parafermions. It is determined by the conformal dimension h^l_m of the parafermionic field that corresponds to the topological sector m, l to be

$$\epsilon^{m,l}_{gs} = \frac{2\pi V_2}{L}h^l_m = \frac{2\pi V_2}{L}\left[\frac{l(l+2)}{4(k+2)} - \frac{m^2}{4k}\right]. \tag{21}$$

As emphasized by Cappelli *et al.* in Refs. 21 and 22, due to the modular invariance of the partition function, the parafermionic characters at high temperature are related to those at low temperature through the modular S matrix. Generally, the characters are a function of the dimensionless variable $\tau = V_2/LT$. Their modular invariance dictates,

$$\chi^l_m(\tau) = \sum_{l'=0}^{k}\sum_{m'=-k}^{k-1} S_{m,l;m',l'}\chi^{l'}_{m'}(1/\tau), \tag{22}$$

where $S_{m,l;m',l'}$ are elements of the modular S matrix,

$$S_{m,l;m',l'} = \frac{1}{\sqrt{k(k+2)}}\sin\frac{\pi(l+1)(l'+1)}{k+2}e^{-i\pi mm'/k}. \tag{23}$$

The high-temperature limit $T \gg \frac{V_2}{L}$ of χ^l_m is then obtained by substituting Eq. (20) into Eq. (22) to get

$$\chi^l_m = \sum_{l'=0}^{k}\sum_{m'=-k}^{k-1} S_{m,l;m',l'}e^{-2\pi TLh^{l'}_{m'}/V_2}. \tag{24}$$

The leading-order contributions in the limit of $T \gg \frac{V_2}{L}$ come from the terms $l'=m'=0$ and $l'=m'=1$ and $l'=-m'=1$. For the former, which we will call "the identity ($\mathbb{1}$) term," $h^0_0=0$. For the latter, which we will call "the quasiparticle term," $h^1_{\pm 1}=\frac{k-1}{2k(k+2)}$. Limiting ourselves to these two terms and substituting Eqs. (23) and (24) in Eq. (19) we can calculate the high-temperature expansion of $Z^l_{n_{is}}$. We find $Z = Z_{\mathbb{1}} + Z_{qp}$ with the two terms corresponding to the identity and quasiparticle contributions, respectively. Since $Z_{\mathbb{1}} \gg Z_{qp}$, we have $\ln Z = \ln Z_{\mathbb{1}} + \frac{Z_{qp}}{Z_{\mathbb{1}}}$. Again, we extract the dependence of $\mathcal{N}$ on A by taking the derivative $\frac{\partial \ln Z}{\partial A}$. Equation (24) limits us to $T \gg V_2/L$ but allows us to calculate both the intermediate ($T \ll V_1/L$) and high ($T \gg V_1/L$) temperature regimes.

In the intermediate temperature regime, Eqs. (14) and (15) hold just as they did for the multicomponent Halperin states but δE_c should be recalculated. Coulomb-blockade peaks are still pronounced, although they are broadened and shifted.

Now, the shift in the charging energy corresponding to the dot having N electrons depends on the quantum number l of the bulk quasiparticles. It is

$$\delta E_c = 4Te^{-2\pi TLh_1^1/V_2}\cos\left(\frac{2\pi N}{k}-\pi\frac{n_{is}}{k}\right)\cos\left(\pi\frac{l+1}{k+2}\right). \tag{25}$$

The suppression factor of the interference, Eq. (3) appears here as determining the shift of the Coulomb-blockade peak.

In the high-temperature regime, the result is similar to Eq. (18). To leading order $\mathcal{N}\approx\nu\frac{BA}{\Phi_0}$. The first correction $\mathcal{N}_1$ has a periodicity that corresponds to the addition of one electron, and is independent of V_2/L. The second correction is the one we are interested in. It is

$$-\frac{2TL}{V_1(k+2)}\cos\left(\pi\frac{l+1}{k+2}\right)e^{-2\pi TLh_1^1/V_2-\pi TL/[V_1k(k+2)]}$$
$$\times\sin\left(\frac{2\pi}{k+2}\frac{BA}{\phi_0}-\pi\frac{n_{is}}{k+2}\right). \tag{26}$$

Again, the dependence of this term on the state of the environment is identical to that found for the lowest-order interference. Furthermore, the thermal suppression factor in Eq. (26) is identical to that found in the limit of lowest-order interference (see Ref. 25 for the $k=2$ case). The high-temperature remainder of the quantization of the charge in the quantum dot is thus found to be intimately connected to the lowest-order interference.

V. SUMMARY

For noninteracting electrons at $\nu=1$, the transition from lowest-order interference in an open Fabry-Perot interferometer to a discrete spectrum in a closed one may be understood by Bohr-Sommerfeld semiclassical arguments. These arguments make it possible to describe the formation of the discrete state through the interference of infinitely many trajectories. This line of thought cannot be immediately applied when interactions are involved and the interferometer is in a fractional quantum Hall state, with quasiparticles that carry a fractional charge. This reasoning is hard to apply for complicated fractional quantum Hall states, where many edge modes coexist. In all these cases, several types of quasiparticles may tunnel across the constriction but the resonances that form when the interferometer closes to be a quantum dot are resonances that correspond to adding or removing electrons.

The behavior of the number of electrons in the interference loop $\mathcal{N}$ as the area, magnetic field and temperature are varied, allows us to explore the universal aspects of the transition, as a function of temperature, from sharp resonances to sinusoidal behavior in an interferometer in the Coulomb-blockaded limit. This is possible since in that limit $\mathcal{N}$ does not depend on the nonuniversal aspects of the two constrictions that form the interferometer, such as the matrix elements for the tunneling of different types of quasiparticles. Rather, it is determined by the partition function, whose modular invariance exposes its universal high-temperature properties. As Eqs. (20) and (24) show, in the Read-Rezayi states, the high-temperature partition function is composed of several leading terms, with each one corresponding to one revolution of the interference loop by one type of quasiparticle, exactly like the lowest-order interference term in an open interferometer. The relative weight between the different quasiparticles is determined by the elements of the modular S matrix and by the thermal suppression of the various terms. The latter, in turn, is determined by the conformal dimensions of the corresponding quasiparticles. The high-temperature partition function of the multicomponent Halperin states, too, is a sum of such terms (see the Appendix below), that can be mapped onto interference of the various types of quasiparticles, each winding once around the interferometer. For both types of states, the thermally smeared Coulomb-blockade peaks carry the same information as the lowest-order interference about the topological properties of the state.

The comparison of the interference and Coulomb-blockade patterns predicted for the Abelian multicomponent Halperin states and the non-Abelian Read-Rezayi states show that when the former are at a symmetry point between the k electronic flavors that compose them, the interferometer cannot distinguish them from the latter. This observation highlights the crucial difference between the two types of states. The properties of the Fabry-Perot interferometer for the non-Abelian states are insensitive to local perturbations to its Hamiltonian while the properties of the Abelian states are modified when local perturbations to its Hamiltonian shift it away from the symmetry point.

Finally, we comment on common experimental values for the parameters we use. The calculations we carry out are valid at temperatures much smaller than the bulk energy gap. For the $\nu=5/2$ state this gap is around 0.5 K. The two velocities V_1 and V_2 were recently calculated numerically by Hu *et al.*,[26] who found $V_2\approx 10^6$ cm/s and $V_1/V_2\approx 7$ for a quantum dot at $\nu=5/2$. The two energy scales V_2/L and V_1/L should be both smaller than the gap, and yet large enough to be within reach of electron cooling. These requirements constrain the dot to be of a circumference of several microns, a scale that is within experimental reach.

ACKNOWLEDGMENTS

We are grateful to Andrea Cappelli for an instructive discussion and for sharing with us unpublished notes. This work was supported by the U.S.-Israel Binational Science Foundation, by the Minerva foundation, by the Einstein center at the Weizmann institute, by Microsoft's Station Q, by NSF under Grant No. DMR-0906475, and by the Heisenberg program of the DFG.

APPENDIX: PARTITION FUNCTION FOR MULTICOMPONENT HALPERIN STATES

1. Canonical ensemble

In this section, we calculate the partition function Z_N for a quantum dot in a multicomponent Halperin state in the canonical ensemble in which the dot has N electrons.

We introduce the abbreviations

$$s_{j,0} \equiv \frac{1}{k+2}\frac{BA}{\Phi_0} + l^{(j)}K^{-1}n = \frac{1}{k+2}\frac{BA}{\Phi_0} - \frac{n_{is}}{2(k+2)} + \frac{1}{2}n_j. \tag{A1}$$

Here, n_j denotes the number of QPs of type j inside the droplet, and $n_{is}=\Sigma_j n_j$ is the total number of QPs. We note that

$$S_0 \equiv \sum_j s_{j,0} = \frac{k}{k+2}\frac{BA}{\Phi_0} + n_{is}\frac{1}{k+2}. \tag{A2}$$

We calculate the canonical partition function by enforcing the constraint of fixed particle number N by a Lagrange multiplier. Then, we perform an unconstrained sum over the set of winding numbers $\{m_i\}$ by applying the Poisson summation formula to each of the sums over winding numbers.

$$\begin{aligned} Z_N &= e^{-(\pi V_1/TL)(N-\Sigma_j s_{j,0})^2}\int d\lambda \sum_{\{s_j\}} e^{-\pi V_2/TL\Sigma_j(s_j-s_{j,0})^2+i\lambda N-i\lambda\Sigma_j s_j} \\ &= \frac{2\pi}{\sqrt{k}}\left(\frac{TL}{V_2}\right)^{k-1/2} e^{-\pi/TL(V_1+V_2/k)(N-\Sigma_j s_{j,0})^2} \\ &\times \sum_{\{p_i\}} \exp\left[\frac{\pi TL}{V_2}\left(\frac{1}{k}\left(\sum_j p_j\right)^2 - \sum_j p_j^2\right)\right. \\ &\left. + \frac{2\pi i}{k}\sum_j p_j\left(N-\sum_l s_{l,0}\right) + 2\pi i\sum_j p_j s_{j,0}\right] \end{aligned} \tag{A3}$$

if $TL/V_2 \gg 1$, leading terms in the partition function have all $p_j \equiv \bar{p}$ equal to each other. The partition function depends on $\bar{p}$ only via a term $\exp(2\pi i\bar{p}N)\equiv 1$. Summing over $\bar{p}$ thus introduces an infinite normalization factor. The origin of this factor is the fact that we introduced k Poisson variables $\{p_j\}$ while only $k-1$ edge charges are freely summed over due to the constraint of fixed total particle number. Having understood the mathematical reason for the appearance of this infinite normalization factor, we discard it and consider $\bar{p}=0$ in the following. We denote the leading term with all $p_j=0$ by

$$Z_N^{(0)} = \frac{2\pi}{\sqrt{k}}\left(\frac{TL}{V_2}\right)^{(k-1)/2} e^{-(\pi/TL)(V_1+V_2/k)(N-\Sigma_j s_{j,0})^2}. \tag{A4}$$

Next, we turn to the subleading terms. The most important of these terms have $p_j=\pm\delta_{j,j_0}$ with $j_0=1,2,\ldots,k$, i.e., one of the $\{p_j\}$ different from zero. Noting that

$$\frac{1}{k}\sum_j \cos(\pi n_j) = I(n), \tag{A5}$$

this contribution reads

$$\begin{aligned} Z_N^{(1)} &= \frac{2\pi}{\sqrt{k}}\left(\frac{TL}{V_2}\right)^{(k-1)/2} e^{-\pi/TL(V_1+V_2/k)(N-\Sigma_j s_{j,0})^2} \\ &\times e^{-(\pi TL/V_2)(1-1/k)} 2kI(n)\cos\left(2\pi\frac{N}{k} - \pi\frac{n_{is}}{k}\right). \end{aligned} \tag{A6}$$

2. Periodicity at intermediate temperatures

We now use the expression (14) to determine the location of the Coulomb-blockade (CB) peak from the requirement $\langle N\rangle = N_0 + \frac{1}{2}$, which corresponds to demanding that the ratio of partition functions $Z_{N_0+1}/Z_{N_0}=1$ is unity. This condition determines the area corresponding to a CB peak as

$$\begin{aligned} A(N_0) = \frac{k+2}{k}\frac{\Phi_0}{B}\left\{N_0 - \frac{n_{is}}{k+2} + \frac{1}{2} + \frac{I(n)TL}{\pi(kV_1+V_2)}\right. \\ \times e^{-\pi TL(k-1)/kV_2}\left[\cos\left(2\pi\frac{N_0+1-n_{is}/2}{k}\right)\right. \\ \left.\left. - \cos\left(2\pi\frac{N_0-n_{is}/2}{k}\right)\right]\right\}. \end{aligned} \tag{A7}$$

When calculating the Fourier transform of a sequence of k consecutive CB peaks with locations according to Eq. (A7), the leading harmonic is determined by the term proportional to $I(n)$ and thus has the same suppression factor as the lowest-order interference.

3. Grand canonical ensemble

In the high-temperature limit, the number of electrons on the dot fluctuates thermally. We now use the results Eqs. (A4) and (A6) to calculate the grand canonical partition function for high temperatures $T \gg V_1/L, V_2/L$. There will be two contributions with a nontrivial area dependence: using the Poisson summation formula to sum $Z_0(N)$ over particle number, the contributions with Poisson index $n=\pm 1$ describe the high-temperature limit of standard CB with a periodicity of one electron. The contribution $Z_1(N)$ on the other hand is already exponentially small in T/V_2, hence it can be integrated over the number of particles and there is no need to use the Poisson summation formula for this term. The area dependence of Eq. (A7) has a period of k electrons. We first calculate the grand canonical generalization of the partition function Eq. (A4). To simplify notation, we use the abbreviation S_0 introduced in Eq. (A2),

$$\begin{aligned} Z_0(\mu) &= \frac{2\pi}{\sqrt{k}}\left(\frac{TL}{V_2}\right)^{(k-1)/2}\sum_N e^{-(\pi/LT)(V_1+V_2/k)(N-S_0)^2+\mu N/T} \\ &\approx \frac{2\pi}{\sqrt{k}}\left(\frac{TL}{V_2}\right)^{(k-1)/2}\sqrt{\frac{TL}{V_1+V_2/k}}e^{\mu^2 L/[4\pi T(V_1+V_2/k)]+\mu S_0/T} \\ &\times\left\{1+e^{-\pi TL/(V_1+V_2/k)}2\cos\left[2\pi\left(S_0\right.\right.\right. \\ &\left.\left.\left.+\frac{\mu L}{2\pi(V_1+V_2/k)}\right)\right]\right\}. \end{aligned} \tag{A8}$$

We next calculate the grand canonical generalization of the partition function Eq. (A6),

$$Z_1(\mu) = 4\pi\sqrt{k}I(n)\left(\frac{TL}{V_2}\right)^{(k-1)/2} e^{-(\pi TL/V_2)(1-1/k)} \int dN e^{-(\pi/LT)(V_1+V_2/k)(N-S_0)^2+\mu N/T} \cos\left(2\pi\frac{N}{k} - \pi\frac{n_{is}}{k}\right)$$

$$= 4\pi\sqrt{k}I(n)\left(\frac{TL}{V_2}\right)^{(k-1)/2} \sqrt{\frac{TL}{V_1+V_2/k}} e^{\mu^2 L/[4\pi T(V_1+V_2/k)]+\mu S_0/T}$$

$$\times e^{-(\pi TL/V_2)(1-1/k)} e^{-(\pi TL)/[k^2(V_1+V_2/k)]} \cos\left[\frac{2\pi}{k}\left(S_0 + \frac{\mu L}{2\pi(V_1+V_2/k)} - \frac{n_{is}}{2}\right)\right]. \tag{A9}$$

Combining the two parts, we find (up to a constant) for the logarithm of the partition function,

$$\ln Z(\mu) = \frac{\mu^2 L}{4\pi T(V_1+V_2/k)} + \frac{\mu S_0}{T} + e^{-\pi TL/(V_1+V_2/k)} 2\cos\left[2\pi\left(S_0 + \frac{\mu L}{2\pi(V_1+V_2/k)}\right)\right]$$

$$+ e^{-\pi TL/[k^2(V_1+V_2/k)]-(\pi TL/V_2)(1-1/k)} 2kI(n)\cos\left[\frac{2\pi}{k}\left(S_0 + \frac{\mu L}{2\pi(V_1+V_2/k)} - \frac{n_{is}}{2}\right)\right]. \tag{A10}$$

The particle number can now be calculated as a derivative $\mathcal{N} = T\frac{\partial}{\partial\mu}\ln Z|_{\mu=0}$.

[1] E. Fradkin, C. Nayak, A. Tsvelik, and F. Wilczek, Nucl. Phys. B **516**, 704 (1998).
[2] A. Stern and B. I. Halperin, Phys. Rev. Lett. **96**, 016802 (2006).
[3] P. Bonderson, A. Kitaev, and K. Shtengel, Phys. Rev. Lett. **96**, 016803 (2006).
[4] P. Bonderson, K. Shtengel, and J. K. Slingerland, Phys. Rev. Lett. **97**, 016401 (2006).
[5] S. B. Chung and M. Stone, Phys. Rev. B **73**, 245311 (2006).
[6] R. Ilan, E. Grosfeld, K. Schoutens, and A. Stern, Phys. Rev. B **79**, 245305 (2009).
[7] R. Ilan, E. Grosfeld, and A. Stern, Phys. Rev. Lett. **100**, 086803 (2008).
[8] R. Willett, L. Pfeiffer, and K. West, Proc. Natl. Acad. Sci. USA **106**, 8853 (2009).
[9] C. de C. Chamon, D. E. Freed, S. A. Kivelson, S. L. Sondhi, and X. G. Wen, Phys. Rev. B **55**, 2331 (1997).
[10] Y. Zhang, D. T. McClure, E. M. Levenson-Falk, C. M. Marcus, L. N. Pfeiffer, and K. W. West, Phys. Rev. B **79**, 241304 (2009).
[11] N. Ofek, A. bid, M. Heiblum, A. Stern, V. Umansky, and D. Mahalu, Proc. Natl. Acad. Sci. USA **107**, 5276 (2010).
[12] B. Rosenow, B. I. Halperin, S. H. Simon, and A. Stern, Phys. Rev. Lett. **100**, 226803 (2008).
[13] B. Rosenow, B. I. Halperin, S. H. Simon, and A. Stern, Phys. Rev. B **80**, 155305 (2009).
[14] W. Bishara, P. Bonderson, C. Nayak, K. Shtengel, and J. K. Slingerland, Phys. Rev. B **80**, 155303 (2009).
[15] P. Bonderson, C. Nayak, and K. Shtengel, Phys. Rev. B **81**, 165308 (2010).
[16] N. Read and E. Rezayi, Phys. Rev. B **59**, 8084 (1999).
[17] X. G. Wen and A. Zee, Phys. Rev. B **46**, 2290 (1992).
[18] G. Moore and N. Read, Nucl. Phys. B **360**, 362 (1991).
[19] M. Levin, B. I. Halperin, and B. Rosenow, Phys. Rev. Lett. **99**, 236806 (2007).
[20] S.-S. Lee, S. Ryu, C. Nayak, and M. P. A. Fisher, Phys. Rev. Lett. **99**, 236807 (2007).
[21] A. Cappelli, G. Viola, and G. Zemba, Ann. Phys. (N.Y.) **325**, 465 (2010).
[22] A. Cappelli, L. Georgiev, and G. Zemba, J. Phys. A: Math. Theor. **42**, 222001 (2009).
[23] B. I. Halperin, Helv. Phys. Acta **56**, 75 (1983).
[24] X. G. Wen, Int. J. Mod. Phys. B **6**, 1711 (1992).
[25] W. Bishara and C. Nayak, Phys. Rev. B **77**, 165302 (2008).
[26] Z.-X. Hu, E. H. Rezayi, X. Wan, and K. Yang, Phys. Rev. B **80**, 235330 (2009).